Rydberg excitation of a single trapped ion

T. Feldker,[1,*] P. Bachor,[1,2] M. Stappel,[1,2] D. Kolbe,[1,2,†] R. Gerritsma,[1] J. Walz,[1,2] and F. Schmidt-Kaler[1]

[1]*Institut für Physik, Johannes Gutenberg-Universität Mainz, Staudingerweg 7, D-55128 Mainz, Germany*[‡]
[2]*Helmholtz-Institut Mainz, Johann-Joachim-Becherweg 36, D-55128 Mainz, Germany*

(Dated: June 22, 2015)

We demonstrate excitation of a single trapped cold $^{40}Ca^{+}$ ion to Rydberg levels by laser radiation in the vacuum-ultraviolet at 122 nm wavelength. Observed resonances are identified as $3d\,^2D_{3/2}$ to 51 F, 52 F and $3d\,^2D_{5/2}$ to 64 F. We model the lineshape and our results imply a large state-dependent coupling to the trapping potential. Rydberg ions are of great interest for future applications in quantum computing and simulation, in which large dipolar interactions are combined with the superb experimental control offered by Paul traps.

PACS numbers: 37.10.Ty, 32.80.Ee, 42.50.Ex

The properties of Rydberg atoms are dominated by one electron being in a state of high principal quantum number, which causes long lifetimes and large dipole moments [1, 2]. This results in giant dipolar interactions between Rydberg atoms [3] which enable the formation of ultralong-range molecules [4], quantum logic gate operations between two neutral atoms [5, 6], and the control of the state of transmitted light through a Rydberg sample at the single photon level [7]. A completely new approach to this field of research is the Rydberg excitation of trapped ions [8, 9, 10], which aims to combine the long-range Rydberg-blockade mechanism, demonstrated in the case of neutral atoms confined in optical lattices [11, 12, 13], with the superb level of control over single ions achieved in Paul traps [14, 15]. Rydberg ions in Coulomb crystals will allow for shaping localized vibrational modes for quantum simulation and fast parallel execution of quantum gates [16, 17]. Further applications are dynamical structural phase transitions and non-equilibrium dynamics driven by Rydberg excitations [18].

Two major challenges have to be met in order to access the unique features of Rydberg ions: Firstly, excitation energies are large compared to the case of neutral atoms such that either a vacuum ultraviolet (VUV) laser source [9, 19] or multi-step excitation [20] with UV lasers is required. Secondly, the large polarizability of Rydberg states makes them very susceptible to residual electric fields in the Paul trap, where an oscillating field with quadrupolar geometry and gradients of about 10^7-10^9 V/m^2 provides stable trapping conditions. Ions are confined near the node (field-zero) of the electric quadrupole, nevertheless residual fields at the position of the ion perturb the Rydberg state and lead to a shifted and broadened resonance.

In this Letter we present laser excitation of a single trapped cold ion to Rydberg states. Ions are initialized in the metastable $3d\,^2D_{3/2}$ or $3d\,^2D_{5/2}$ state before they are excited to the 51 F and 52 F (from $D_{3/2}$) respectivly 64 F (from $D_{5/2}$) state using vacuum ultraviolet radiation near 122 nm. By applying a state dependent fluorescence measurement following the decay of the Rydberg state, population transfer out of the initial D-state is detected. The polarizability of the Rydberg ion is deduced from the observed line-shift and -broadening,

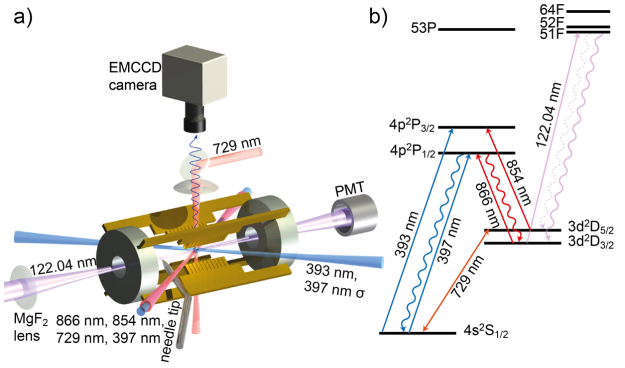

FIG. 1. a) Sketch of the x-shaped ion trap (B) with two segmented gold-covered DC blades and two RF blades. Laser beams near 397 nm, 866 nm, 854 nm, 393 nm and 729 nm can be switched and serve for cooling, optical pumping and state analysis. Fluorescence light near 397 nm is collected by a lens with numerical aperture NA = 0.27 and imaged on an electron-multiplying charge-coupled device (EMCCD) camera. Holes in the endcaps provide access for the VUV beam. The VUV beam intensity is monitored with a photomultiplier tube (PMT). A sharp tip can be moved into the trap for aligning the VUV beam. b) Levels and transitions in $^{40}Ca^{+}$. Ions are cooled on the $S_{1/2}$ to $P_{1/2}$ transition near 397 nm with optical pumping on the $D_{3/2}$ to $P_{1/2}$ transition at 866 nm and initialized for the Rydberg excitation by optical pumping into the $D_{3/2}$ ($D_{5/2}$) level with light near 397 nm (393 nm).

caused by residual electric fields in the trap.

Experiments were carried out in two different linear Paul traps. Trap (A) consists of four cylindrical rods with diameter d = 2.5 mm at a diagonal distance of 2.2 mm, and two endcaps at a distance of 10 mm [9, 21]. It has a rather large trapping volume and features stable ion trapping at very low field gradients. Trap (B) is constructed from x-shaped gold-covered blades at a diagonal distance of 0.96 mm, see ref. [22], and Fig. 1 a. Axial confinement is provided by applying voltages to the segments of the DC blades. The improved design of this trap allows for a more precise alignment of the electrodes. Thus residual fields at the ion are reduced and the trap can be operated at higher vibrational frequencies compared to trap (A). Ions are loaded from a thermal beam of neutral calcium atoms by photoionization with laser light near 423 nm and 375 nm. Trapped ions are illuminated by laser radiation

near 397 nm and 866 nm for optical cooling and fluorescence detection with an electron-multiplying charge-coupled device (EMCCD) camera. Additional laser beams at 393 nm, 854 nm and 729 nm allow for optical pumping, sideband spectroscopy and coherent manipulation of the $4s\,^2S_{1/2}$ - $3d^2\,D_{5/2}$ transition, respectively.

Figure 1 b shows relevant energy levels of the calcium ion. The Rydberg transition is driven by VUV single-photon excitation at 122 nm wavelength from the metastable $D_{3/2}$ and $D_{5/2}$ levels. To generate continuous-wave coherent VUV radiation we employ four-wave sum-frequency mixing in mercury vapor. Power levels in the μW range are achieved using a triple-resonant scheme with fundmental light fields at 254 nm, 408 nm and 555 nm which are generated by frequency-doubling and -quadrupling of lasers in the near infrared [9, 19]. The wavelength of these lasers are monitored by a wavelength meter (HighFinesse WSU-10), which is calibrated to the $4s\,^2S_{1/2}$ - $3d^2\,D_{5/2}$ transition and thus accurate to about 100 MHz at the sum frequency. The VUV radiation is focused on the ion by a pair of MgF_2 lenses and the transmitted power is monitored by a photomultiplier tube (PMT). For a precise determination of the focus we use a sharp tip which can be temporarily moved into the trap and monitor the transmission of the VUV beam. The beam is aligned by shifting one of the MgF_2 lenses as well as the ion traps vacuum vessel which is mounted on a translation stage.

We search Rydberg resonances at wavelengths near 122.04 nm, where the efficiency of the four-wave mixing process is strongly enhanced by the nearby $7\,^1S$-$11\,^1P$ resonance in mercury. Inital information about the expected resonances [23] could not be reproduced, and uncertainties of theory predictions [9] are too large, so that we had to search the full range of about 180 GHz between Rydberg states of consecutive principle quantum number.

The ion is excited to the Rydberg state in a sequence of steps: i) Initialization by optical pumping to the $3d^2\,D_{3/2}$ state (lifetime: 1176(11) ms [24]). ii) VUV excitation by a 30 ms pulse. The Rydberg state then decays and within 30 ms is either back in the initial state, or the $3d^2\,D_{5/2}$ (lifetime: 1168(9) ms [24]), or the ground state $4s^2\,S_{1/2}$ and the detection efficiency is therefore dominated by the branching fractions out of the initial state. iii) For the detection, ground state population is optically pumped into the $D_{5/2}$ state with resonant light at 393 nm (90% efficiency from the branching ratio to the $D_{3/2}$ level). iv) Under resonant excitation with laser light at 397 nm and 866 nm the ion emits no fluorecence light, if the Rydberg excitation in (ii) was successful. Figure 2 a shows the observed resonance. For the data shown in Fig. 2 b, the pumping step (iii) is omitted in order to prove that this Rydberg state is decaying into the D-states.

We observe Rydberg excitation to the 51 F state at 122.041 913(5) nm and to the 52 F state at 122.032 384(10) nm wavelength. The linewidth of the excitation to the 51 F varies between 60 MHz and 400 MHz full-width at half-maximum (FWHM), depending on the trap control parameters. Similar measurements have been

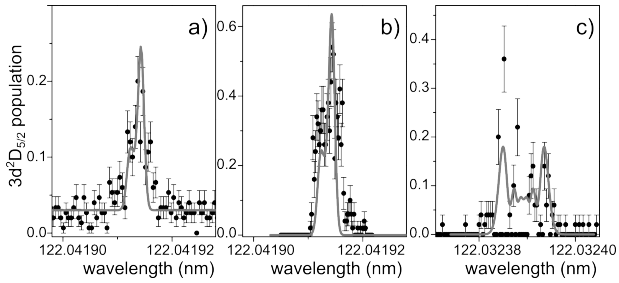

FIG. 2. a) and b): Rydberg excitation from the $3d^2\,D_{3/2}$ to the 51 F state, at a VUV power of 0.5 μW and 30 ms pulse duration. The trap (A) is operated at motional frequencies of $\omega_{ax,rad}/(2\pi) = 90, 200$ kHz. a) Ground state population is optically pumped to the $3d^2\,D_{5/2}$ state after the Rydberg excitation. The linewidth is $\simeq$ 60 MHz full-width-at-half-maximum (FWHM). b) No optical pumping, only the direct decay to $3d^2\,D_{5/2}$ is observed. This data confirmes that the Rydberg level is a F-state (see text for details). c) Excitation from the $3d^2\,D_{3/2}$ to the 52 F state in trap (B), operated at motional frequencies of $\omega_{ax,rad}/(2\pi) = 270, 700$ kHz. The line shape model includes broadening by thermal excitation, magnetic field, micromotion and Stark effect. 50 single shot measurements were taken for each datapoint, the errorbars depict the quantum projection noise.

carried out with linear three and five-ion crystals. For the F resonances the branching ratio between the decay from the Rydberg state into the $D_{5/2}$ and $D_{3/2}$ state is estimated to be about 7 %, using data from lower-lying Rydberg states (cf. NIST atomic spectra database). The decay of a Rydberg F-state into the $S_{1/2}$ state is forbidden.

In addition, Rydberg excitation to the 64 F state starting from the $3d^2\,D_{5/2}$ state is observed at 122.040 50(5) nm. The resonance width is larger, about 1 GHz, as the state is at the edge of being stable in the trap [8, 9]. Consequently, the 64 F state is not measured by applying the electron shelving scheme as described above, but by observation of a significantly increased ion loss rate on resonance. Ion loss is also observed, albeit less frequently, for the 51 F and 52 F resonances in $\sim 0.3\%$ of the Rydberg excitations.

Energy levels for Rydberg states are given by

$$E_{n,\delta} = -\frac{R_\infty}{1+\frac{m_e}{m_{\mathrm{ca}^+}}} \times \frac{Z^2}{(n-\delta)^2} \qquad (1)$$

where R_∞ is the Rydberg constant, m_e is the electron mass, m_{ca^+} is the mass of the calcium ion, Z is the charge-state, and n is the principal quantum number. δ denotes the quantum defect and values from theory [8] are δ_F = 0.026 and δ_P = 1.44 for F- and P-states, respectively. Measured energy differences are consistent with a nearly vanishing quantum defect (F-state excitation) and principal quantum num-

state	**wavelength from $D_{3/2}$**	**wavelength from $D_{5/2}$**	**ΔE cm^{-1}**
51F	122.041 913(5) nm	–	95589.258(3)
52F	122.032 384(10) nm	–	95595.656(7)
64F	–	122.040 50(5) nm	95650.901(33)

TABLE I. Levels, transition vacuum wavelengths, and energies from the $S_{1/2}$ ground state.

bers of n = 51, n = 52 and n = 64. Table 1 shows the transition frequencies and energies determined. Measured frequencies of 411.042 129 776 393 THz for the $4s^2\,S_{1/2}$ to $3d^2\,D_{5/2}$ transition [25] and 1.819 599 021 504 THz for the $3d^2\,D_{5/2}$ - $3d^2\,D_{3/2}$ fine structure splitting [26] have been used in the data analysis. The identification of the resonances is supported by the fact that decay from the Rydberg F-states is mainly into the $3d\,^2D$ states as observed experimentally (see Fig. 2 b), in contrast to Rydberg P-states which would predominatly decay into the $4s^2\,S_{1/2}$ state [27].

In order to model the observed resonance lines, the electric field, the motional state of the ion and the magnetic field are taken into account: The electric field at the position of the ion is determined from the micromotion line-broadening of the $4s\,^2S_{1/2} - 4p\,^2P_{3/2}$ transition. Due to fabrication imperfections in the geometry of trap (A), the ion is exposed to an alternating electric field proportional to the trap drive amplitude $E_{Ion} \propto U_{RF} \times \sin(\Omega t)$, where U_{RF} is the applied radiofrequency voltage at the trap-driving frequency $\Omega/2\pi$. This causes micromotion in the axial direction along the VUV laser beam, which leads to a modulation of the Rydberg energy due to the electric polarizability α, and –in addition– to a modulation of the Doppler effect. The instantenous resonance frequency reads:

$$\omega(t) = \omega_0 + k x_{mm} \Omega \sin \Omega t - \frac{\alpha E_{ion}^2}{2} \cos^2 \Omega t. \qquad (2)$$

Here, ω_0 is the bare resonance frequency, k is the wavenumber of the laser along the motion of the ion, E_{ion} is the electric field amplitude and x_{mm} is the micromotion amplitude. From this equation we can derive the temporal shape of the resonance laser field

$$\begin{aligned} E_{res}(t) \propto\; & e^{-i\omega_0 t} e^{i2\beta_\alpha \Omega t} \\ & \times \sum_n J_n(\beta_{mm})\, e^{in(\Omega t + \frac{\pi}{2})} \\ & \times \sum_m (-1)^m J_m(\beta_\alpha)\, e^{2im\Omega t}. \end{aligned} \qquad (3)$$

In this equation we define the modulation index in the Bessel functions $J_n(\beta)$ due to the axial micromotion by $\beta_{mm} = k x_{mm}$ and due to the oscillating Stark shift by $\beta_\alpha = \alpha E_{ion}^2/8\Omega$. The second exponent in Eq. (3) denotes a static frequency shift due to the fact that the modulated Stark shift can only reduce the transition frequency to the F states. It is apearant that the lineshape comes from a complicated interplay from the sidebands at $n\times\,\Omega_{rf}$ caused by the micromotion and the sidebands at $2n\times\,\Omega_{rf}$ caused by the oscillating Stark shift. Thermal ion motion at T ≈ 5 mK and the magnetic field of B = 0.45 mT, as determined from sideband spectroscopy of the $4s\,^2S_{1/2}$ - $3d\,^2D_{5/2}$ transition, are leading to a broadening of ≈ 10 MHz, preventing us from resolving the sidebands.

In trap (B), residual electric fields are generated by charging the surface of the trap electrodes with VUV radiation. The resulting field is thus pointing in the radial direction and linebroading by micromotion parallel to the axial aligned VUV beam is negligible while the Stark effect remains the dominant line broadening effect.

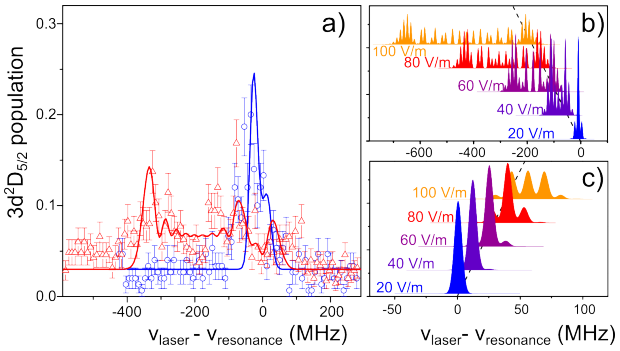

FIG. 3. a) Experimental data (trap A) of the $3d\,^2D_{3/2}$ to 51 F resonance with E_{Ion} = 24 V/m (blue) and 84 V/m (red). Fitting the data with our lineshape model, we determine $\alpha_{51F}/2$ = 5×10^2 MHz/(V/cm)^2 for the polarizability. 50 single shot measurements were taken for each datapoint, the errorbars depict the quantum projection noise. b) Calculated lineshapes for the $D_{3/2}$ to 51 F transition at different residual electric fields. The axial micromotion is neglected (trap B) and cooling to the Doppler limit is assumed. Features of this calculation are compatible with experimental data. c) Set of lineshapes for the transition $D_{3/2}$ to 51 P with the same parameters as in b). Features of this calculation are incompatible with experimental data. This observation corroborates the indentification of the excited Rydberg levels as F-states.

With the known electric field amplitude E_{Ion} we determine α from the fit of the observed resonance line shape, the data is presented in Fig. 3 a. Calculated lineshapes at various electric fields for the transitions to the 51F- and 51P-state are presented in Fig. 3 b and c, the polarizabilities used in the calculation are estimated from second-order perturbation theory whith neglected spin-orbit coupling. We use the quantum defects found in [8] and the method developed in [28] to obtain analytical approximate wavefunctions for computing matrix elements. As a check to the accuracy of this approach, we compare the calculated lifetime of the 4P state of 6.55 ns, to the experimental value of 7 ns, which agrees reasonably well. In the second-order perturbation theory, we set $m_L = 0$, which is justified as this state experiences the largest Stark shift for the states of interest. In the calculation, we take couplings to the states $n = 40, .., 60$ into account, which was found to lead to convergence.

The experimentally determined $\alpha/2 = 5\times10^2$ MHz/(V/cm)^2 is close to the polarizability of the 51 F state, $\alpha_{51F}/2 \approx 4\times10^2$ MHz/(V/cm)^2 obtained from second-order pertubation theory and neglecting spin-orbit coupling. Under the assumption that the Rydberg level is the 51 P state the determined electric polarizability would be inconsistent with the theoretical value of $\alpha_{51P}/2 \approx -37\times$ MHz/(V/cm)^2 from ref. [29]. Again, this supports the identifiction of the Rydberg levels as F-states.

In both traps we have observed that Rydberg excitation becomes unstable after several months of experimenting. We

conjecture surface contamination (e.g. calcium from the loading atomic beam) and VUV generated photo electrons to be the reason for this observation and plan to use a dedicated ion-loading zone well separated from the spectroscopy zone [30, 31] to avoid VUV-induced photoemission of electrons and charging of electrodes. In the future increased VUV power and tighter focussing will allow for significantly higher excitation rates. This should enable the excitation of Rydberg P-states, where the dipole matrix elements are lower by about one order of magnitude. Much narrower excitation resonances are expected from Rydberg P-states, because the electric polarizability is lower, $\alpha_P/\alpha_F \simeq 0.1$. For a single ion in the motional ground state, and exposed to residual electric field of 65 V/m as measured from the Rydberg resonance in Trap (B), we expect a modulation index of 0.6. This results in a strong carrier and resolved sidebands at a frequency of $\pm 2\times\Omega_{rf}$ weaker by a factor of three. In view of driving coherent dynamics, we note that already with the achieved values for VUV power of 3 μW and a focussing of 10 μm, Rabi frequencies of up to $2\pi\times$ 150 kHz for the transition $3\mathrm{d}\,^2\mathrm{D}_{3/2}$ to 52 P are expected [9], which is much faster than the natural decay of 217 μs [32].

In conclusion we have observed and identified Rydberg excitations of a single cold ion and measured the lineshape of the resonance which implies a strong state-dependent coupling to the electric trapping potential. This experimental work is a starting point for establishing a novel platform of Rydberg matter, where the unique possibilities of state dependent electric forces as well as long-range dipole-dipole interactions are combined with the outstanding control over quantum states in trapped ion cyrstals.

Acknowledgments The authors acknowledge helpful discussions with W. Li, I. Lesanovsky, P. Zoller and M. Drewsen. We acknowledge G. Jakob and S. Wolf for support with the assembly of trap (B). This work was funded by the BmBF and the chist-era network(R-ION consortium) and by the European Union H2020 FET Proactive project RySQ (grant N. 640378).

* feldker@uni-mainz.de
† Present address: Institut für Technische Physik, Deutsches Zentrum für Luft- und Raumfahrt, Pfaffenwaldring 38-40, D-70569 Stuttgart, Germany
‡ http://www.quantenbit.de

[1] J. M. Raimond, M. Brune, and S. Haroche, *Rev. Mod. Phys.* **73,** 565-582 (2001).
[2] M. Saffman, T. Walker, and K. Mølmer, *Rev. Mod. Phys.* **82,** 2313–2363 (2010).
[3] M. D. Lukin, M. Fleischhauer, R. Cote, L. M. Duan, D. Jaksch, J. I. Cirac, and P. Zoller, *Phys. Rev. Lett.* **87,** 037901 (2001).
[4] V. Bendkowsky, B. Butscher, J. Nipper, J. P. Shaffer, R. Löw, and T. Pfau, *Nature* **458,** 1005–1009 (2009).
[5] T. Wilk, A. Gaëtan, C. Evellin, J. Wolters, Y. Miroshnychenko, P. Grangier, and A. Browaeys, *Phys. Rev. Lett.* **104,** 010502 (2010).
[6] L. Isenhower, E. Urban, X. L. Zhang, A. T. Gill, T. Henage, T. A. Johnson, T. G. Walker, and M. Saffman, *Phys. Rev. Lett.* **104,** 010503 (2010).
[7] T. Peyronel, O. Firstenberg, Q. Y. Liang, S. Hofferberth, A. V. Gorshkov, T. Pohl, M. D. Lukin, and V. Vuletic, *Nature* **488,** 57–60 (2012).
[8] M. Müller, L. Liang, I. Lesanowsky, and P. Zoller, *New J. Phys.* **10,** 093009 (2008).
[9] F. Schmidt-Kaler, T. Feldker, D. Kolbe, J. Walz, M. Müller, P. Zoller, W. Li, and I. Lesanovsky, *New J. Phys.* **13,** 075014 (2011).
[10] W. Li, and I. Lesanovsky, *Appl. Phys. B* **114,** 37–44 (2014).
[11] T. Amthor, C. Giese, C. S. Hofmann, M. Weidemüller, *Phys. Rev. Lett.* **104,** 013001 (2010).
[12] P. Schauß, M. Cheneau, M. Endres, T. Fukuhara, S. Hild, A. Omran, T. Pohl, C. Gross, S. Kuhr, and I. Bloch, *Nature* **491,** 87–91 (2012).
[13] S. Ravets, H. Labuhn, D. Barredo, L. Béguin, T. Lahaye, and A. Browaeys, *Nature Physics* **10,** 914-917 (2014).
[14] P. O. Schmidt, T. Rosenband, C. Langer, W. M. Itano, J. C. Bergquist, and D. J. Wineland, *Science* **309**, 749–752 (2005).
[15] R. Blatt, and C. F. Roos, *Nature Physics* **8,** 277–284 (2012).
[16] W. Li, A. W. Glaetzle, R. Nath, and I. Lesanovsky, *Phys. Rev. A* **87,** 052304 (2013).
[17] R. Nath, M. Dalmonte, A. W. Glaetzle, P. Zoller, F. Schmidt-Kaler, and R. Gerritsma, *arXive:1504.01474* (2015).
[18] W. Li, and I. Lesanovsky, *Phys. Rev. Lett.* **108,** 023003 (2012).
[19] D. Kolbe, M. Scheid, and J. Walz, *Phys. Rev. Lett.* **109,** 063901 (2012).
[20] M. Hennrich, Univ. Innsbruck, Austria: private communication
[21] T. Feldker, L. Pelzer, M. Stappel, P. Bachor, R. Steinborn, D. Kolbe, J. Walz, and F. Schmidt-Kaler, *Appl. Phys. B.* **114,** 11–16 (2014).
[22] G. Jacob, K. Groot-Berning, S. Wolf, S. Ulm, L. Couturier, U. G. Poschinger, F. Schmidt-Kaler, and K. Singer, arXiv:1405.6480 (2014).
[23] C. B. Xu, X. P. Xie, R. C. Zhao, W. Sun, P. Xue, Z. P. Zhong, W. Huang, and X. Y. Xu, *J. Phys. B* **31,** 5355–5360 (1998).
[24] A. Kreuter, C. Becher, G. P. T. Lancaster, A. B. Mundt, C. Russo, H. Häffner, C. Roos, W. Hänsel, F. Schmidt-Kaler, R. Blatt, and M. S. Safronova *Phys. Rev. A* **71,** 032504 (2005).
[25] M. Chwalla, J. Benhelm, K. Kim, G. Kirchmair, T. Monz, M. Riebe, P. Schindler, A. S. Villar, W. Hänsel, C. F. Roos, R. Blatt, M. Abgrall, G. Santarelli, G. D. Rovera, and Ph. Laurent, *Phys. Rev. Lett.* **102,** 023002 (2009).
[26] R. Yamazaki, H. Sawamura, K. Toyoda, S. Urabe, *Phys. Rev. A* **77,** 012508 (2008).
[27] W. Li, Univ. Nottingham, U.K.: private communication
[28] V. A. Kostelecký, and M. M. Nieto, *Phys. Rev. A* **32,** 3243–3246 (1985).
[29] A. A. Kamenski, and V. D. Ovsiannikov, *J. Phys. B* **47** 095002 (2014).
[30] J. Home, D. Hanneke, J. D. Jost, J. M. Amini, D. Leibfried, and D. J. Wineland, *Science* **325,** 1227–1230 (2009).
[31] T. Ruster, C. Warschburger, H. Kaufmann, C. T. Schmiegelow, A. Walther, M. Hettrich, A. Pfister, V. Kaushal, F. Schmidt-Kaler, and U. G. Poschinger, *Phys. Rev. A* **90,** 033410 (2014)
[32] I. L. Glukhov, E. A. Nikitina, and V. D. Ovsiannikov, *Opt. Spectrosc.* **115,** 9–17 (2013).